J. Electr. Electron. Mater.
Vol. 38, No. 5, pp. 546-553 September 2025
doi: https://doi.org/10.4313/JEEM.2025.38.5.10
ISSN 1226-7945(Print), 2288-3258(Online)

Regular Paper

Dielectric Properties of High-capacity BME MLCCs via $(Na_{0.5}Bi_{0.5})TiO_3$ as a Rare-Earth-Free Dopant

Change-Ho Lee and Jung Rag Yoon
R & D Center, Samwha Capacitor, Yongin 17118, Korea

(Received May 6, 2025; Revised May 27, 2025; Accepted May 27, 2025)

Abstract: In this study, the dielectric and electrical properties of high-capacitance base metal electrode (BME) multilayer ceramic capacitors (MLCCs) fabricated using a $BaTiO_3$–MgO–Mn_3O_4–$(Na_{0.5}Bi_{0.5})TiO_3$ (NBT)–$(BaCa)SiO_3$ dielectric system were investigated under reducing atmospheres with oxygen partial pressures (PO_2) ranging from 10^{-10} to 10^{-12} MPa. By incorporating NBT, the dielectric performance remained stable across the entire range of reducing atmospheres. The fabricated MLCCs exhibited consistent capacitance values, low dielectric loss (<2.8%), and high insulation resistance, reaching up to 2.4 GΩ at 25°C and 0.675 GΩ at 125°C. Furthermore, excellent breakdown voltage performance (up to 550 V at 25°C) and Class II-compatible temperature coefficient of capacitance (TCC) behavior were observed, meeting the X8R specification. The $BaTiO_3$–MgO–Mn_3O_4–NBT–$(BaCa)SiO_3$ dielectric system demonstrates that NBT can serve as a promising alternative to conventional rare-earth dopants in BME MLCCs, enabling excellent thermal and electrical stability, high capacitance, and long-term reliability even under reducing conditions. These results confirm the feasibility of developing cost-effective, sustainable, and rare-earth-free MLCCs for high-performance applications in automotive, industrial, and energy storage systems.

Keywords: $BaTiO_3$, $(Na_{0.5}Bi_{0.5})TiO_3$, BME MLCC, X8R

1. INTRODUCTION

Multilayer ceramic capacitors (MLCCs) are essential passive components in modern electronic devices, offering high capacitance, stability, and reliability. In particular, high-capacitance MLCCs are crucial for automotive electronic systems, industrial electronics, and energy storage applications, where stable operation is required under high temperatures and harsh environments [1-3]. Base metal electrode (BME) MLCCs with high capacitance and thermal stability are typically fabricated using $BaTiO_3$-based dielectrics and Ni or Cu internal electrodes through a sintering process in a reducing atmosphere. To stabilize the crystal structure of $BaTiO_3$-based dielectrics and optimize dielectric properties under such conditions, dopants such as Mn, Mg, V and Cr, along with rare-earth elements such as Dy, Y, and Ho, have been commonly used. These rare-earth elements play a critical role in improving the reliability and temperature coefficient of capacitance (TCC) through A-site and B-site substitution and core-shell structure formation. Additionally, due to factors such as oxygen vacancy control, lattice stability enhancement, and domain structure adjustment, these elements significantly enhance the DC-bias characteristics and lifespan of BME MLCCs [4-7]. However, rising costs and supply chain instabilities associated with rare-earth elements have driven interest in alternative dielectric materials that can achieve equivalent or superior performance without reliance on rare-earth dopants. Recent studies have focused on incorporating $(Na_{0.5}Bi_{0.5})TiO_3$ (NBT), a perovskite-structured

✉ **Jung Rag Yoon; yoonjungrag@samwha.com**

Copyright ©2025 KIEEME. All rights reserved.
This is an Open-Access article distributed under the terms of the Creative Commons Attribution Non-Commercial License (http://creativecommons.org/licenses/by-nc/3.0) which permits unrestricted non-commercial use, distribution, and reproduction in any medium, provided the original work is properly cited.

material with a high curie temperature of approximately 320°C, into $BaTiO_3$-based dielectrics. The goal of this approach is to achieve superior dielectric properties and core-shell structure formation, effectively replacing rare-earth dopants [8-10]. When NBT is added to $BaTiO_3$, Na^+ and Bi^{3+} partially substitute Ba^{2+} and Ti^{4+} within the lattice due to their similar ionic radii, minimizing changes in tetragonality and maximizing dielectric polarization. The simultaneous A-site and B-site substitution also results in the presence of acceptor and donor states, which contribute to charge compensation and enhance dielectric properties. Furthermore, the incorporation of Bi^{3+} suppresses oxygen vacancy formation, thereby improving long-term electrical reliability and reducing temperature-dependent permittivity variations. In this study, BME MLCCs were fabricated and their electrical properties evaluated using a modified composition, in which the rare-earth elements (Y_2O_3, Dy_2O_3) in the conventional high-capacitance BME MLCC system based on $BaTiO_3$-MgO-Mn_3O_4-(BaCa)SiO_3 [11-13] were replaced with NBT. Previous studies have examined the dielectric and electrical characteristics of MLCCs incorporating Co, Ta, and Ho into the $BaTiO_3$-NBT composition [14-17]. However, in most cases, noble metals such as Ag and Ag-Pd have been used as internal electrodes, and sintering has been performed in an oxidative atmosphere. In contrast, this study investigates the characteristics of BME MLCCs with NBT additives replacing rare-earth elements under a reducing atmosphere. Given that the oxygen partial pressure (PO_2) during sintering in a reducing environment significantly affects the formation of oxygen vacancies, variations in donor/acceptor concentrations, and the electrical properties of ceramics, this study explores these effects in detail.

2. EXPERIMENTAL

2.1 Fabrication of MLCC Samples

In this study, to fabricate high-capacitance BME MLCCs, dielectric materials suitable for sintering under a reducing atmosphere were employed. The dielectric composition was primarily based on $BaTiO_3$ (KCM, Japan), with MgO, Mn_3O_4, V_2O_5, NBT, and (BaCa)SiO_3 glass powders used as additives. NBT powder was synthesized via the conventional solid-state reaction method using Na_2CO_3 (99.9%, High Purity Chemicals, Japan), Bi_2O_3 (99.9%, High Purity Chemicals, Japan), and TiO_2 (99.8%, Aldrich) as starting materials. These raw materials were weighed according to the stoichiometric ratio and ball-milled with ethanol and zirconia balls for 24 hours. The slurry was then dried at 80°C for 24 hours. The dried powder was calcined at 800°C for 4 hours and subsequently pulverized for use. The $BaTiO_3$-MgO-Mn_3O_4-V_2O_5-NBT-(BaCa)SiO_3 powders were mixed and dispersed with PVB (Sekisui, BM-SZ), ethanol/toluene, and DOP (DC Chemical) using a Nano-set Mill to prepare a homogeneous slurry. The prepared slurry was cast into 14 μm thick sheets on a release PET film using a slot die coater. After casting, Ni internal electrodes were screen-printed onto the green sheets. A total of 90 layers were laminated to form a multilayer bar. The laminated bars were then subjected to cold isostatic pressing, followed by cutting into individual green chips using a cutter. The green chips underwent binder burnout (BBO) at 240°C for 72 hours. Sintering was then carried out at 1150°C for 2 hours under a reducing atmosphere, with an oxygen partial pressure (pO_2) in the range of 10^{-10} to 10^{-12} MPa. To control the pO_2 during the BME MLCC sintering process, a mixture of H_2 and N_2 gases was passed through water vapor, and the resulting pO_2 was regulated based on the equilibrium between H_2 and H_2O. A reoxidation treatment was subsequently carried out at 900°C for 60 minutes under a mildly oxidative atmosphere (PO_2= 10^{-7} MPa). After polishing the sintered chips, Cu external electrodes were applied and heat-treated at 800°C to complete the fabrication of MLCCs with final dimensions of 3.2 mm (W) × 1.6 mm (L) × 1.6 mm (T).

2.2 Evaluation of Dielectric Properties and Microstructure

The dielectric properties of the MLCC samples were characterized using an LCR meter (Keysight E4980A) at a frequency of 1.0 kHz and an AC signal amplitude of 1.0 Vrms to measure capacitance and dissipation factor. The C–V characteristics were obtained by combining the same LCR meter with a DC power supply (Keysight E3643A). Insulation resistance (IR) was measured using a high resistance meter (HP 4339B) after applying a DC voltage of 4 V/μm for 60 seconds. The breakdown voltage per unit thickness was evaluated using a dielectric withstand tester (HIOKI 3174).

During this test, a DC voltage was applied at a ramp rate of 0.5 V/s in a temperature chamber until the leakage current reached 1 μA, which was defined as the breakdown threshold. The temperature coefficient of capacitance (TCC) was evaluated over the temperature range from –25°C to 125°C at a frequency of 1 kHz, using an LCR meter (HP 4284A) placed in a temperature-controlled chamber. Stepwise insulation resistance (Step-IR) measurements were conducted at 25°C, 85°C, and 125°C using a DC power supply, a digital electrometer, and a high-temperature shielded chamber. The microstructural characteristics of the MLCC samples were analyzed using field-emission scanning electron microscopy (FE-SEM, JSM-9701, JEOL).

3. RESULTS AND DISCUSSION

Figure 1 shows the variation in capacitance and dielectric loss of a $BaTiO_3$–MgO–Mn_3O_4–NBT–(BaCa)SiO_3 based MLCCs as a function of hydrogen concentration. The oxygen partial pressure (PO_2) was controlled by adjusting the H_2/H_2O ratio, while the dew point of the H_2O humidifier was maintained at 38 ~ 40°C. As a result, the PO_2 was estimated to be in the range of approximately 10^{-10} to 10^{-12} MPa. The capacitance was observed to decrease significantly from 890 nF to 770 nF as the hydrogen concentration increased. Generally, in MLCCs, capacitance is influenced by both the dielectric constant and the electrode coverage under identical design conditions. In this study, the change in electrode coverage due to the hydrogen atmosphere was negligible; therefore, the reduction in capacitance is attributed to a decrease in dielectric constant from approximately 2,718 to 2,448. As the hydrogen concentration increased, hydrogen acted as a strong reducing agent during sintering, leading to the partial reduction of Ti^{4+} to Ti^{3+} in the $BaTiO_3$ lattice. This reduction generated oxygen vacancies and induced lattice distortion. Such defects interfere with the formation of ferroelectric domains, ultimately resulting in a reduction in the dielectric constant. The observed decrease in capacitance under a hydrogen-rich atmosphere is thus considered to result from a combination of changes in Ti^{3+} concentration, which affects both electronic and ionic polarization, and the suppression of domain formation. Meanwhile, dielectric loss was measured to be in the range of 2.14% to 2.8%, demonstrating excellent performance within the 5% limit required for Class II MLCCs. Furthermore, dielectric loss tended to decrease gradually as hydrogen concentration increased. Although Ti^{3+} ions typically act as charge carriers that contribute to increased dielectric loss, an excessive concentration of Ti^{3+} can hinder domain wall motion and reduce overall capacitance, which in turn leads to a decrease in AC dielectric loss. This explains the observed trend in dielectric behavior under reducing conditions.

Figure 2 illustrates the insulation resistance characteristics

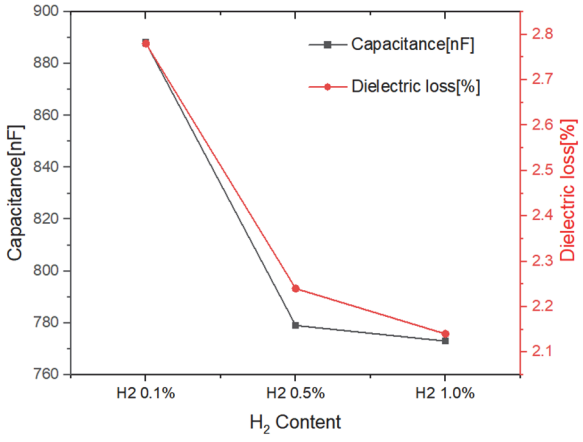

Fig. 1. Capacitance and dielectric loss of a $BaTiO_3$–MgO–Mn_3O_4–NBT–(BaCa)SiO_3 based MLCCs as a function of hydrogen concentration.

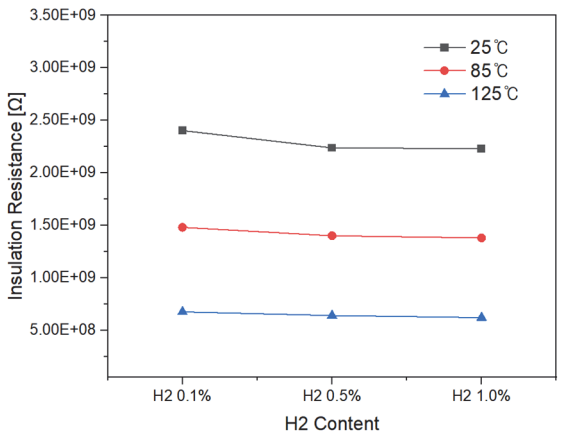

Fig. 2. Insulation resistance characteristics of the $BaTiO_3$–MgO–Mn_3O_4–NBT–(BaCa)SiO_3 based MLCCs as a function of hydrogen concentration and measurement temperature.

of the $BaTiO_3$–MgO–Mn_3O_4–NBT–$(BaCa)SiO_3$ based MLCCs as a function of hydrogen concentration and measurement temperature. Even in the absence of rare-earth element doping, the insulation resistance at 25°C ranges from 2.22 to 2.4 GΩ, indicating excellent dielectric insulation performance. At high temperatures (125°C), the insulation resistance remains between 0.62 and 0.675 GΩ, meeting the reliability standards required for Class II MLCCs. In general, for $BaTiO_3$-based high-permittivity ceramics sintered under reducing atmospheres, the lack of donor or acceptor dopants typically results in the formation of oxygen vacancies, leading to a significant degradation of insulation resistance, often dropping below 1 MΩ at high temperatures. However, in the present study, excellent insulation performance was achieved even without rare-earth dopants, suggesting that the addition of NBT alone can effectively compensate for the electrical degradation typically observed under such conditions. It has been reported that rare-earth dopants such as Dy, Y, and Ho can selectively substitute into the A-site or B-site of the $BaTiO_3$ perovskite structure, as described by the defect reactions in Equation (1). When occupying the A-site, these dopants behave as donors, whereas substitution into the B-site results in acceptor-like behavior, both mechanisms contributing to improved insulation resistance [18].

$$\text{A-site substitution : } R_2O_3 \rightarrow 2R_{Ba'} + V_{Ba''} + 3O_O \quad (1)$$

$$\text{B-site substitution : } R_2O_3 \rightarrow 2R_{Ti'} + 2O_O + V_{O''}$$

In the case of NBT, which functions as a substitute for rare-earth additives, Na^+ and Bi^{3+} ions primarily occupy the A-site, while Ti^{4+} occupies the B-site. It is presumed that Na^+ and Bi^{3+} substitute into A-site lattice positions and act as donor species, generating oxygen vacancies to compensate for the induced charge imbalance. This defect chemistry mechanism is believed to be the principal contributor to the enhanced insulation resistance, rather than changes induced by the sintering atmosphere [19].

Figure 3 illustrates the breakdown voltage of the $BaTiO_3$–MgO–Mn_3O_4–NBT–$(BaCa)SiO_3$ based MLCCs as a function of hydrogen concentration and measurement temperature. As the hydrogen content increases, the breakdown voltage at 25°C decreases from 550 V to 475 V. In general, the breakdown voltage tends to decrease with increasing measurement temperature, showing a particularly sharp drop from 330 V to 275 V at 125°C. At a hydrogen concentration of 0.1%, the dielectric withstand strength is approximately 70 V/μm at 25 °C, which is comparable to that of conventional MLCCs. The observed decrease in breakdown voltage with increasing hydrogen content is attributed to the formation of oxygen vacancies, which can combine with electrons or Ti^{3+} ions to create leakage paths, significantly deteriorating the insulation properties. Furthermore, as the temperature increases, leakage current rises, leading to electric field concentration and localized heating. This ultimately results in thermal runaway, which further contributes to the reduction in breakdown voltage.

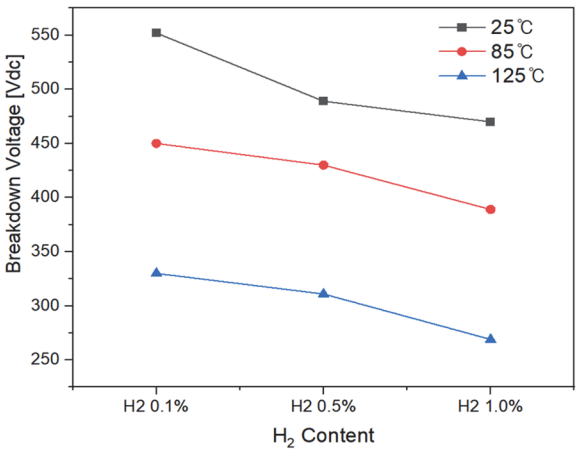

Fig. 3. Breakdown voltage of the $BaTiO_3$–MgO–Mn_3O_4–NBT–$(BaCa)SiO_3$ based MLCCs as a function of hydrogen concentration and measurement temperature.

Figure 4 illustrates the FE-SEM micrographs of the $BaTiO_3$–MgO–Mn_3O_4–NBT–$(BaCa)SiO_3$ based MLCCs as a function of hydrogen concentration. Figure 4(a) shows the microstructure of an MLCC with a hydrogen content of 0.5%, where the dielectric layer thickness is approximately 9 μm and the internal electrode thickness is about 1.15 μm. No deformation is observed in either the electrodes or the dielectric layers. Figure 4(b), 4(c), and 4(d) present the microstructures at varying hydrogen concentrations. While the grain size remains relatively consistent regardless of hydrogen content, an increase in secondary phase-like grains is observed with higher hydrogen concentrations. To investigate these secondary phases, Fig. 5 presents the EDS (energy-dispersive X-ray spectroscopy) analysis of an MLCC with 0.5% hydrogen

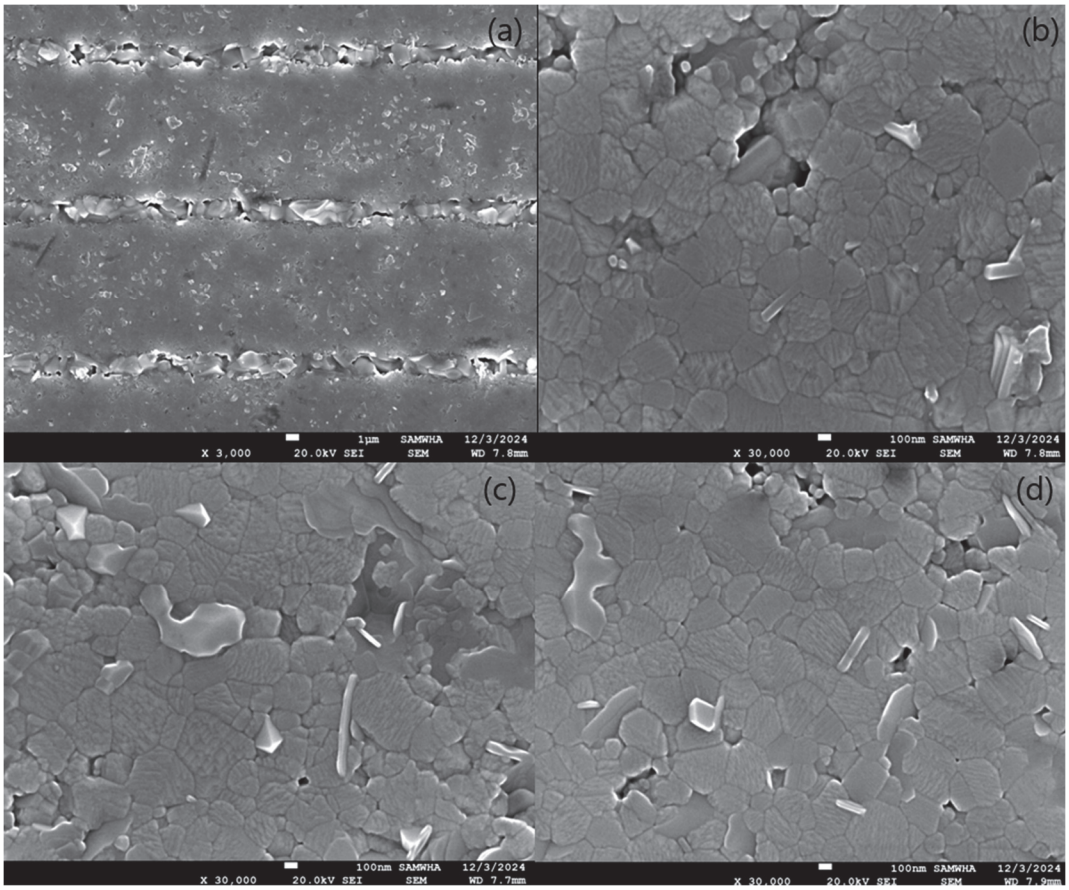

Fig. 4. SEM micrographs of the $BaTiO_3$–MgO–Mn_3O_4–NBT–(BaCa)SiO_3 based MLCCs as a function of hydrogen concentration. (a) Microstructure of MLCC, (b) H_2 0.1%, (c) H_2 0.5%, and (d) H_2 1.0%.

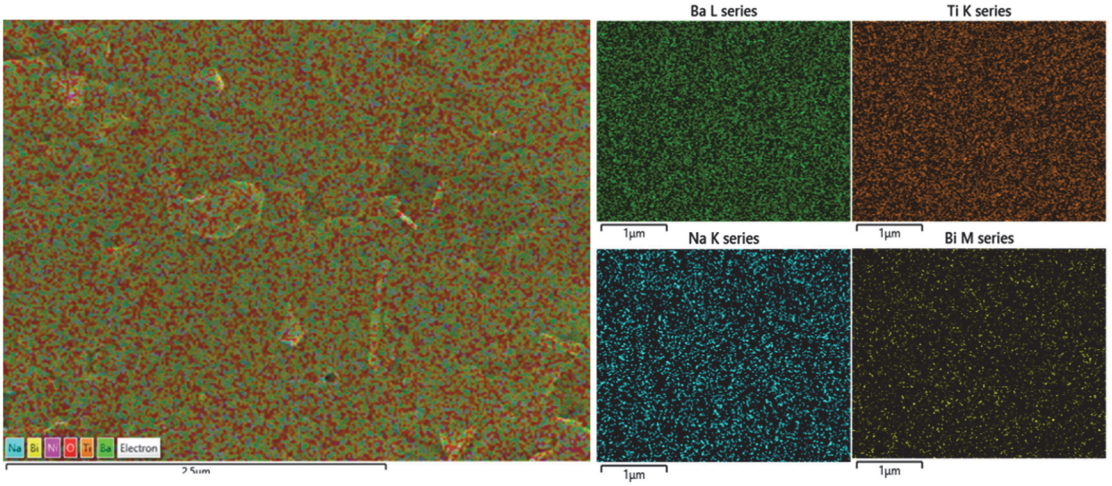

Fig. 5. EDX analysis of the $BaTiO_3$–MgO–Mn_3O_4–NBT–(BaCa)SiO_3 based MLCCs with 0.5% hydrogen content.

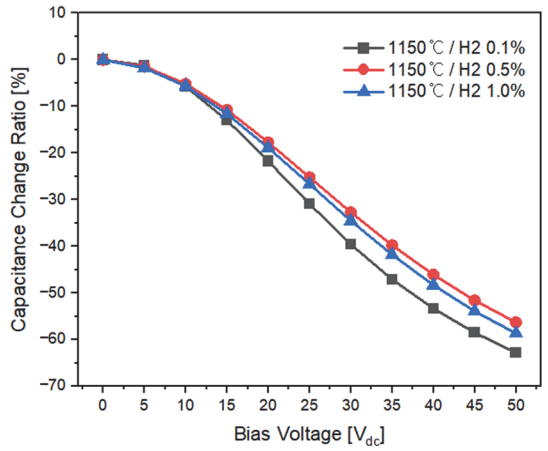

Fig. 6. Capacitance–voltage (C–V) characteristics of the $BaTiO_3$–MgO–Mn_3O_4–NBT–$(BaCa)SiO_3$ based MLCCs as a function of hydrogen concentration.

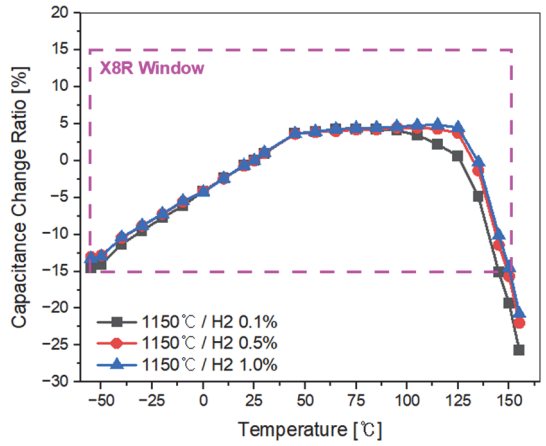

Fig. 7. TCC characteristics of the $BaTiO_3$–MgO–Mn_3O_4–NBT–$(BaCa)SiO_3$ based MLCCs as a function of hydrogen concentration.

content. The results indicate a uniform distribution of Ba, Ti, Bi, and Na ions throughout the matrix. Moreover, no significant compositional differences in Bi or Na were found within the grains that appear to correspond to the secondary phases.

Figure 6 illustrates the capacitance–voltage (C–V) characteristics of the $BaTiO_3$–MgO–Mn_3O_4–NBT–$(BaCa)SiO_3$ based MLCCs as a function of hydrogen concentration. MLCCs with high dielectric constants typically exhibit nonlinear C–V behavior, wherein the capacitance decreases with increasing applied voltage due to domain reorientation under the electric field. This reduction in dielectric permittivity leads to a corresponding decrease in effective capacitance, which can pose challenges in precision analog circuits and power supply applications. As the hydrogen concentration increases, the rate of capacitance change with respect to voltage becomes more gradual, indicating improved voltage stability. This trend is consistent with the dielectric behavior observed in Fig. 1. In high-permittivity systems, strong electric fields tend to saturate domain wall motion, which contributes to increased polarization nonlinearity. Nevertheless, the system demonstrates C–V characteristics comparable to those of conventional MLCCs, despite the absence of rare-earth elements in its composition [20].

Figure 7 illustrates the TCC characteristics, showing that the curie temperature of $BaTiO_3$ shifts upon the addition of NBT, with a suppressed dielectric peak. This results in MLCC performance that meets the X8R specification, where capacitance variation remains within ±15% over the temperature range of -55°C to 125°C. In general, the mechanism for improving the TCC in BME MLCCs is attributed to the behavior of $BaTiO_3$, which exhibits ferroelectric properties at room temperature and undergoes phase transitions with temperature variations, resulting in significant changes in dielectric permittivity.

To mitigate this behavior, rare-earth elements such as Dy and Y are typically doped to modify the phase transition temperature and to control domain wall motion, thereby tuning the curie temperature and achieving a more stable TCC response over a wide temperature range [18,20]. Similar effects have been observed with NBT doping, where the Curie temperature of $BaTiO_3$ shifts to a higher temperature and the dielectric peak becomes less pronounced [9,10,16]. Furthermore, with increasing hydrogen content, the TCC behavior becomes more flattened and the variation in dielectric permittivity at elevated temperatures is reduced. This behavior is considered to originate from the same mechanism observed in the dielectric response presented in Fig. 1.

Figure 8 presents the insulation resistance–voltage (IR–V) characteristics of the $BaTiO_3$–MgO–Mn_3O_4–NBT–$(BaCa)SiO_3$-based MLCCs with 0.5% hydrogen content, measured as a function of temperature. Variations in insulation resistance with respect to applied voltage and temperature are critical indicators of electrochemical degradation mechanisms in BME MLCCs, such as oxygen vacancy migration and electromigration, and play a key role in lifetime assessment [20,21]. The IR–V measurements reveal that insulation

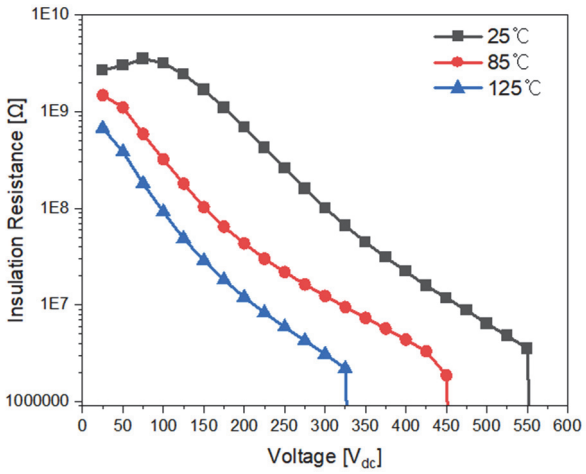

Fig. 8. Insulation resistance–voltage (IR–V) characteristics of the $BaTiO_3$–MgO–Mn_3O_4–NBT–(BaCa)SiO_3-based MLCCs with 0.5% hydrogen content as a function of test temperature.

resistance decreases with increasing temperature and voltage. When compared to conventional BME MLCCs rated at 50 V, the developed MLCC exhibits stable performance, maintaining an insulation resistance of 0.18 GΩ at 125°C and a breakdown voltage approximately 6.5 times higher than its rated voltage. These results indicate superior electrical stability and robustness under high-temperature and high-voltage conditions.

4. CONCLUSION

In this study, BME MLCCs were successfully fabricated using a $BaTiO_3$–MgO–Mn_3O_4–$(Na_{0.5}Bi_{0.5})TiO_3$–(BaCa)SiO_3 dielectric system without the use of rare-earth dopants. The incorporation of NBT effectively stabilized the dielectric properties under reducing atmospheres. The fabricated MLCCs exhibited stable capacitance, low dielectric loss (<2.8%), and high insulation resistance, achieving values of up to 2.4 GΩ at 25°C and 0.675 GΩ at 125°C. Moreover, excellent breakdown voltage performance (up to 550 V at 25°C) and a TCC compatible with Class II specifications were observed, satisfying the requirements of the X8R standard. The enhanced thermal stability is attributed to NBT's ability to shift and flatten the curie peak, thereby compensating for the functionality typically provided by rare-earth dopants. Furthermore, C–V measurements demonstrated voltage stability comparable to conventional MLCCs, while IR–V characteristics confirmed high reliability under high-temperature and high-voltage stress conditions. In conclusion, the newly developed $BaTiO_3$–MgO–Mn_3O_4–NBT–(BaCa)SiO_3 dielectric system demonstrates that NBT is a promising alternative to rare-earth dopants in BME MLCCs, offering superior thermal and electrical stability, high capacitance, and long-term reliability. These results represent a significant advancement in the development of cost-effective, sustainable, and rare-earth-free MLCCs for high-performance applications in automotive, industrial, and energy storage systems.

ORCID

Jung Rag Yoon https://orcid.org/0000-0002-9206-8701

ACKNOWLEDGMENTS

This work was supported by the Technology Innovation Program (RS-2024-00430833, Development of MLCC commercialization technology for automotive electronics an alternative to rare earth for high reliability response) funded by the Ministry of Trade, Industry & Energy (MOTIE, Korea).

REFERENCES

[1] H. Yang, W. Bao, Z. Lu, L. Li, H. Ji, Y. Huang, F. Xu, G. Wang, and D. Wang, *J Mater Res*., **36**, 1285 (2021). doi: https://doi.org/10.1557/jmr.2020.286

[2] I. Seo, H. Y. Kim, H. W. Kang, C. M. Oh, S. H. Han, and H. Kim, *J. Korean Inst. Electr. Electron. Mater. Eng*., **38**, 132 (2025). doi: https://doi.org/10.4313/JKEM.2025.38.2.2

[3] T. Kim, M. K. Kim, J. R. Yoon, J. Y. Lee, O. Seok, and M. W. Ha, *J. Electr. Eng. Technol*., **20**, 1103 (2025). doi: https://doi.org/10.1007/s42835-025-02156-y

[4] K. Hong, T. H. Lee, J. M. Suh, J. S. Park, H. S. Kwon, J. Choi, and H. W. Jang, *Electron. Mater. Lett*., **14**, 629 (2018). doi: https://doi.org/10.1007/s13391-018-0066-6

[5] C. H. Lee and J. R. Yoon, *J. Ceram. Process. Res*., **23**, 794 (2022). doi: https://doi.org/10.36410/jcpr.2022.23.6.794

[6] T. Okamoto, S. Kitagawa, N. Inoue, and A. Ando, *Appl. Phys. Lett*., **98**, 072905 (2011). doi: https://doi.org/10.1063/1.3555466

[7] C. H. Lee and R. Y. Jung, *J. Korean Inst. Electr and Electron. Mater. Eng*., **38**, 161 (2025).

doi: https://doi.org/10.4313/JKEM.2025.38.2.5

[8] L. Chen, H. Wang, P. Zhao, C. Zhu, Z. Cai, Z. Cen, L. Li, and X. Wang, *J. Am. Ceram. Soc*., **102**, 4178 (2019).
doi: https://doi.org/10.1111/jace.16292

[9] Y. Sun, H. Liu, H. Hao, L. Zhang, and S. Zhang, *Ceram. Int*., **41**, 931 (2015).
doi: https://doi.org/10.1016/j.ceramint.2014.08.140

[10] S. F. Wang, Y. F. Hsu, Y. W. Hung, and Y. X. Liu, *Appl. Sci.*, **5**, 1221. (2015).
doi: https://doi.org/10.3390/APP5041221

[11] C. H. Lee and J. R. Yoon, *J. Ceram. Process. Res*., **24**, 588 (2023).
doi: https://doi.org/10.36410/jcpr.2023.24.3.588

[12] S. H. Lee, D. Y. Kim, M. K. Kim, H. K. Kim, J. H. Lee, E. Baek, and J. R. Yoon, *J. Ceram. Process. Res*, **16**, 495 (2015).
doi: https://doi.org/10.36410/jcpr.2015.16.5.495

[13] J. Chun, J. Heo, K. S. Lee, B. U. Ye, B. S. Kang, and S. H. Yoon, *Sci Rep*., **14**, 616 (2024).
doi: https://doi.org/10.1038/s41598-024-51254-w

[14] Z. Shen, X. Wang, and L. Li, *J. Mater. Sci. Mater. Electron.*, **28,** 3768 (2017).
doi: https://doi.org/10.1007/s10854-016-5986-z

[15] L. Chen, K. Hui, H. Wang, P. Zhao, L. Li, and X. Wang, *J. Eur. Ceram. Soc.* **39**, 3710 (2019).
doi: https://doi.org/10.1016/j.jeurceramsoc.2019.05.041

[16] Y. Li, N. Fan, J. Wu, B. Xu, X. Li, X. Liu, Y. Xiao, D. Hou, X. Feng, J. Zhang, S. Zhang, J. Li, and F. Li, *Nat. Commun.*, **15**, 8958 (2024).
doi: https://doi.org/10.1038/s41467-024-53287-1

[17] H. I. Hsiang, L. T. Mei, and Y. J. Chun, *J. Am. Ceram. Soc.* **92**, 2768 (2009).
doi: https://doi.org/10.1111/j.1551-2916.2009.03245.x

[18] K. J. Park, C. H. Kim, Y. J. Yoon, S. M. Song, Y. T. Kim and K. H. Hur, *J. Eur. Ceram. Soc*., **29**,1735 (2009).
doi: https://doi.org/10.1016/j.jeurceramsoc.2008.10.021

[19] H. S. Lee and J. R. Yoon, *J. Korean Inst. Electr. Electron. Mater. Eng*., **37**, 662 (2024).
doi: https://doi.org/10.4313/JKEM.2024.37.6.13

[20] D. Y. Jeong, S. I. Lee, H. Y. Lee, M. K. Kim, and J. R. Yoon, *Jpn. J. Appl. Phys.*, **52**, 10MB23 (2013).
doi: https://doi.org/10.7567/JJAP.52.10MB23

[21] J. R. Yoon, K. M. Lee, and S. W. Lee, *Trans. Electr. Electron. Mater*., **10**, 5 (2009).
doi: https://doi.org/10.4313/TEEM.2009.10.1.005